



Gazi University

**Journal of Science**

PART A: ENGINEERING AND INNOVATION

<http://dergipark.org.tr/guj.1565477>

## Shielding Behaviour of TiO<sub>2</sub> Reinforced Composite Materials Against 4 MeV Energy Photons and Neutrons

Zübeyde ÖZKAN<sup>1\*</sup> Uğur GÖKMEN<sup>2</sup> <sup>1</sup> Department of Advanced Technologies, Graduate School of Natural and Applied Sciences, Gazi University, Ankara, Türkiye<sup>2</sup> Department of Metallurgical and Materials Engineering, Faculty of Technology, Gazi University, Ankara, Türkiye

Keywords	Abstract
Al 6068 TiO <sub>2</sub> Gamma Shielding Fast Neutron Shielding	In order to eliminate or minimize the possible negative effects that may arise due to the use of increased artificial radiation, the radiation permeability properties of Al 6082 alloy material, Al 6082+5% TiO <sub>2</sub> , Al+15% TiO <sub>2</sub> , and Al 6082+25% TiO <sub>2</sub> metal matrix composite materials against 4 MeV fast neutron and gamma radiation were analyzed in the NGCal program. Mass attenuation coefficient (MAC), mean free path (MFP), linear attenuation coefficient (LAC), tenth value layer (TVL), and half value layer (HVL) and parameters were analyzed for both fast neutron and gamma radiation. As a result of the analysis of 4 MeV energy fast neutron and gamma radiation, the linear attenuation values of the material against both fast neutron and photon increased depending on the increasing reinforcement ratio, while the half value layer, tenth value layer and mean free path values decreased. While the LAC values of Al 6082, Al 6082+5% TiO <sub>2</sub> , Al+15% TiO <sub>2</sub> , Al 6082+25% TiO <sub>2</sub> materials against fast neutrons vary between approximately 0.00074 cm <sup>-1</sup> and 0.0173 cm <sup>-1</sup> , their LAC values against photons vary between 0.084 cm <sup>-1</sup> and 0.96 cm <sup>-1</sup> .
Cite	
	Özkan, Z., & Gökmen, U. (2024). Shielding Behaviour of TiO <sub>2</sub> Reinforced Composite Materials Against 4 MeV Energy Photons and Neutrons. <i>GU J Sci, Part A, 11(4)</i> , 722-731. doi:10.54287/guj.1565477
Author ID (ORCID Number)	Article Process
0000-0003-2901-7749	Zübeyde ÖZKAN
0000-0002-6903-0297	Uğur GÖKMEN
	<b>Submission Date</b> 11.10.2024 <b>Revision Date</b> 11.11.2024 <b>Accepted Date</b> 23.11.2024 <b>Published Date</b> 30.12.2024

### 1. INTRODUCTION

With the spread of radiation such as X-ray, electron, beta, proton, gamma, neutron, and alpha, the field of radiation technologies has become increasingly widespread in recent years. Nuclear radiation is used in science, neutron capture therapy, agriculture, medicine, nuclear power plants, industry, and material inspection. Gamma rays are high-energy and intense ionizing radiation because they have short wavelengths and the highest frequencies in the electromagnetic spectrum. Neutrons are uncharged particles that are often used in nuclear reactors to produce nuclear, plant mutation breeding, cancer therapy, neutron imaging, neutron activation analysis, and neutron microscopy. Because they are uncharged, they easily pass through the material and react with the nucleus of the target atom. Although the basic theory of neutron shielding is known, the radiation shielding process is more complex than gamma rays due to its wide energy range. The most frequently used materials for neutron shielding in theoretical and experimental studies conducted by many researchers are; concrete, boron-containing compounds such as polyethylene, gadolinium, cadmium heavy metals, boron, boron nitrides, boron oxide, boron carbide, etc. (Reda & Saled, 2021; Chang et al., 2023). Radiation protective materials are barriers designed to protect against various negative effects caused by radiation. They reduce the amount of dose that individuals are exposed to by attenuating or absorbing radiation.

\*Corresponding Author, e-mail: [zubeydeozkan@gazi.edu.tr](mailto:zubeydeozkan@gazi.edu.tr)

Among the Mo–TiO<sub>2</sub>, TiO<sub>2</sub>, and Co–TiO<sub>2</sub> nanocomposite materials produced by Mahmoud et al. (2024) and his colleagues, the Co–TiO<sub>2</sub> composite obtained a LAC value of 0.845 cm<sup>-1</sup> at 0.1 MeV energy and the best shielding material at 0.1 MeV energy was the Co–TiO<sub>2</sub> composite. Jandaghian et al. (2024) designed a radiation shield for the ARGUS reactor. They found that the 180 cm thick shielding material they designed from barite concrete was better than the 230 cm thick polyethylene shielding material. In their studies examining the shielding properties of tellurium glasses against 100 kGy and 50 kGy, Juhim et al. (2023) determined that the Al<sub>2</sub>O<sub>3</sub> ceramic added to tellurium increased the MAC value of tellurium glasses. Huo et al. (2024) in their studies investigating the gamma and neutron shielding properties of Sm<sub>2</sub>O<sub>3</sub> filled polymer composite materials, found that Sm<sub>2</sub>O<sub>3</sub> filling improved the radiation shielding properties of the composite material. Aldawood et al. (2024) in study to determine the radiation properties of Ti6Al4V alloy reinforced polymer composite materials with Ti6Al4V alloy reinforcement ratios ranging from 20-50% by weight, found that the LAC value of the material increased with increasing reinforcement ratio. Almuqrin et al. (2023) found that MoO<sub>3</sub> reinforced C<sub>2</sub>H<sub>4</sub> composites, which they investigated as an alternative material to concrete, showed better shielding properties than concrete at energies of 32.5 keV, 40.3 keV and 36.5 keV. Akman et al. (2021) as a result of experimental and theoretical gamma analysis of polymer composite materials reinforced with 5-10-15% FeCr, found that the shielding properties of the materials improved with increasing FeCr ratio. Huwayz et al. (2024) in their studies investigating the effect of BaO on the radiation shielding properties of SiO<sub>2</sub>-B<sub>2</sub>O<sub>3</sub>-SrO-ZrO<sub>2</sub>, found that the materials they produced were better than many conventional concrete materials and recently advanced glasses. Eke (2024), found that as the amount of WO<sub>3</sub> in the glass material incremented, the radiation shielding properties improved in his study of the effect of WO<sub>3</sub> on ZnO-Na<sub>2</sub>O-B<sub>2</sub>O<sub>3</sub> glasses. Nafee et al. (2024) investigated the X-ray shielding properties of polymer composite materials with different ZnO and CdO concentrations and found that the TVL value of the composite materials they manufactured was lower than that of gypsum and concrete materials.

In the literature, many different materials are being investigated by many researchers, combining different types of materials (composite, Mg alloys, ceramics, glass, super alloys etc.), to be used as alternative materials to traditional materials. In this study, a composite material was designed to be an alternative material to traditional materials in shielding both fast neutron and gamma radiation. The Al 6082 matrix material in the Al 6xxx series, whose strength value can be increased by adding reinforcement materials, will be reinforced with TiO<sub>2</sub> ceramic material at 5%, 15% and 25% and the radiation permeability of the Al 60682 alloy, the tenth value layer (TVL), mass attenuation coefficient (MAC), mean free path (MFP), half value layer (HVL), and linear attenuation coefficient (LAC) parameters in neutron and gamma sources will be examined and analyzed in the NGCal program.

## 2. MATERIAL AND METHOD

NGCal, an online software (Gökçe et al., 2021), enables the theoretical calculation of MAC, LAC, HVL, TVL, MFP parameters that describe the shielding properties of compounds, elements and composite materials exposed to fast neutrons (4 MeV), thermal neutrons (25.4 meV) and photons (gamma and X-rays). It performs analysis in the range of 0.002 MeV photon energy to 20 MeV photon energy. Thanks to the program, information can be entered without restricting the content of oxides, carbides, etc. found in alloys and composite materials with mixed chemical composition.

The units and formulas of the parameters used are given in Table 1. Information including matrix/reinforcement ratios and codes of the analyzed materials is given in Table 2.

**Table 1.** Information on shielding parameters

Parameters	Formulas	Units	References
<b>Linear attenuation coefficient (LAC)</b>	$I = I_0 e^{-\mu x}$	cm <sup>-1</sup>	(Alım et al., 2022)
<b>Mass attenuation coefficient (MAC)</b>	$\mu_m = \frac{\mu}{\rho}$	cm <sup>2</sup> /g	(Kılıçoğlu & Tekin, 2020)
<b>Half value layer (HVL)</b>	$HVL = \frac{\ln(2)}{\mu}$	cm	(Kavun et al., 2022)
<b>Tenth value layer (TVL)</b>	$TVL = \frac{\ln(10)}{\mu}$	cm	(Kılıçoğlu & Tekin, 2020)
<b>Mean free path (MFP)</b>	$MFP = \frac{1}{\mu}$	cm	(Kavun et al., 2022)

**I:** Intensity after passing through material  
**I<sub>0</sub>:** Initial intensity before entering material  
**μ:** Linear attenuation coefficient  
**x:** Thick of the material  
**ρ:** Density

**Table 2.** Materials chemical composition

Name of the sample	Composition
<b>T0</b>	Al 6082
<b>T5</b>	Al 6082+5% TiO <sub>2</sub>
<b>T15</b>	Al 6082+15% TiO <sub>2</sub>
<b>T25</b>	Al 6082+25% TiO <sub>2</sub>

### 3. RESULTS

#### LAC

Linear attenuation coefficients against photons and fast neutrons with 4 MeV energy The LAC values of the samples coded T0-T5-T15-T25 are given in Figure 1. In the face of a photon with 4 MeV energy; The LAC value of the material has raised because of increasing TiO<sub>2</sub>. The reason for this is that the higher the density and atomic number of the shielding material, the higher the probability of attenuating the incoming photon. This is because the atomic numbers of the Ti (22) and O (8) atoms that make up the TiO<sub>2</sub> ceramic material are higher than the atomic numbers of Al (13), which is the main material of the Al 6082 alloy, and that TiO<sub>2</sub> ceramics is higher than Al 6082. A neutron with an energy above 1 MeV is called a fast neutron. Absorption of fast neutrons is practically impossible, therefore, to stop a fast neutron, its energy must first be reduced to the level of thermal neutrons fewer than 0.025 eV (first step - attenuation), and then such thermalized neutrons are captured (second step - absorption) (Piotrowski, 2021). The LAC values of the samples coded T0-T5-T15-T25 in the face of a fast neutron with 4 MeV energy; the LAC value of the material has raised due to increasing TiO<sub>2</sub>.

This is because fast neutrons interact more with the shielding material as they pass through dense materials, causing them to lose their energy. When the graph is examined, the LAC values of the T0-T5-T15-T25 coded materials against gamma are higher than the LAC value of the fast neutron. The reason for this is; gamma rays are a type of electromagnetic radiation. They lose their energy with the gamma shielding material by photoelectric effect (PE), pair production (PP) and Compton scattering (CS). Neutrons are electrically neutral particles. Neutrons can interact with the shielding material through various processes, these processes include scattering, thermalization, absorption and nuclear reactions. For these reasons, they have different LAC values despite having the same energies.

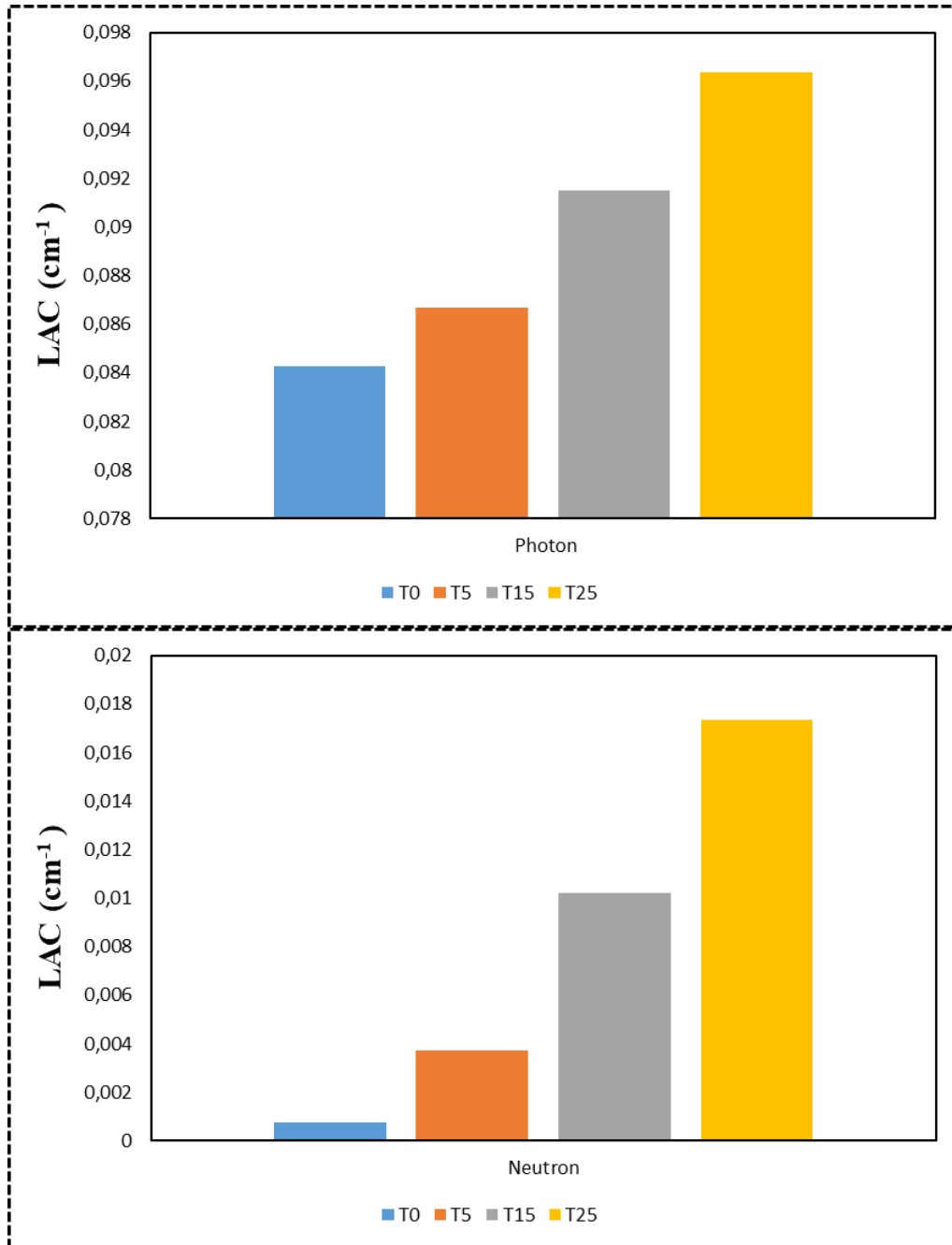


**Figure 1.** LAC graphs of samples coded T0-T5-T15-T25

## MAC

The MAC values of the T0-T5-T15-T25 coded samples against photons and fast neutrons with 4 MeV energy are given in Figure 2. Depending on the decreasing TiO<sub>2</sub> ratio, the MAC values of the materials against both photons and fast neutrons do not decrease. The MAC values of the T0-T5-T15-T25 coded samples against fast neutrons are approximately 0.000274 cm<sup>2</sup>/g; 0.00134 cm<sup>2</sup>/g; 0.00348 cm<sup>2</sup>/g; 0.0056 cm<sup>2</sup>/g, respectively. Against photons, they have taken the values of approximately 0.031 cm<sup>2</sup>/g; 0.03111 cm<sup>2</sup>/g; 0.03114 cm<sup>2</sup>/g; 0.03118 cm<sup>2</sup>/g, respectively. Because the LAC values of the materials against photons are higher than the LAC values against neutrons, the MAC values of photons are higher. The addition of TiO<sub>2</sub> to Al 6082 caused increases in the density values of composite materials. The higher the number of atoms per unit volume in materials with high density, the higher the possibility of fast neutrons interacting.

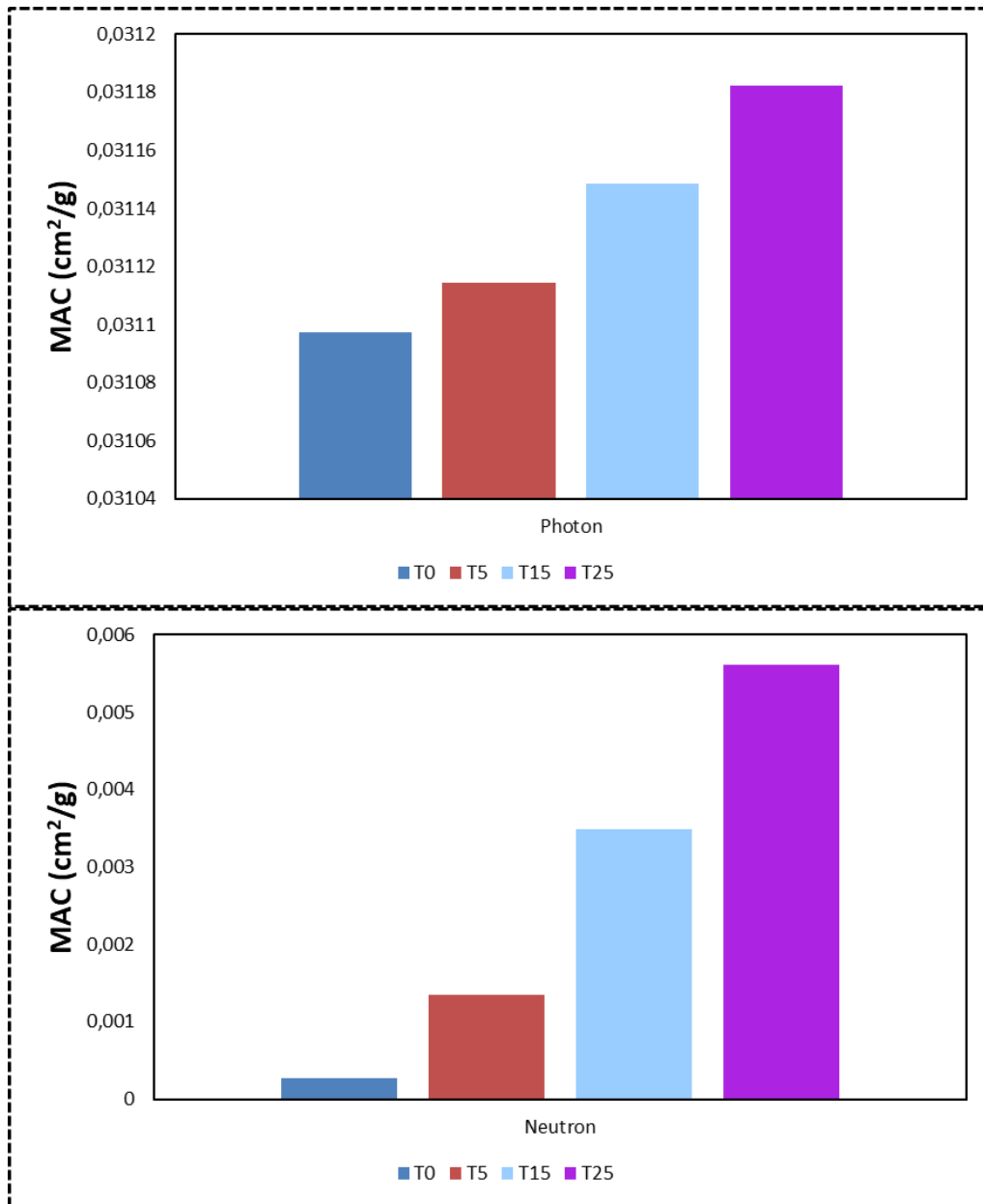


*Figure 2. MAC graphs of samples coded T0-T5-T15-T25*

## TVL

The HVL values of the T0-T5-T15-T25 coded samples against 4 MeV energy photons and fast neutrons are given in Figure 3. In the face of 4 MeV energy photons; the HVL value of the material decreased due to increasing TiO<sub>2</sub>. As a result of adding 25% TiO<sub>2</sub> into Al 6082, the HVL value against 4 MeV neutron energy decreased by approximately 95.7%. This provided a significant decrease in the material thickness required for the Al 6082 material to be a neutron shielding material with the addition of TiO<sub>2</sub>. The thickness values of the materials to be used as neutron and gamma shielding materials are very important parameters in terms of usability, manufacturability and cost. For this reason, the addition of TiO<sub>2</sub> increased the possibility of the material being usable as a neutron shielding material. Decreases occurred in the TVL values of the T0-T5-T15-T25 coded samples due to the increasing TiO<sub>2</sub> ratio against 4 MeV energy photons. However, the decrease in TVL values due to the increase in TiO<sub>2</sub> is not as clear and sharp as the neutron TVL values. The addition of 25% TiO<sub>2</sub> to Al 6082 caused a decrease of approximately 12.5% in TVL values. When photons interact with material, they could lose an important amount of energy in an interaction, causing their intensity to decrease more rapidly.

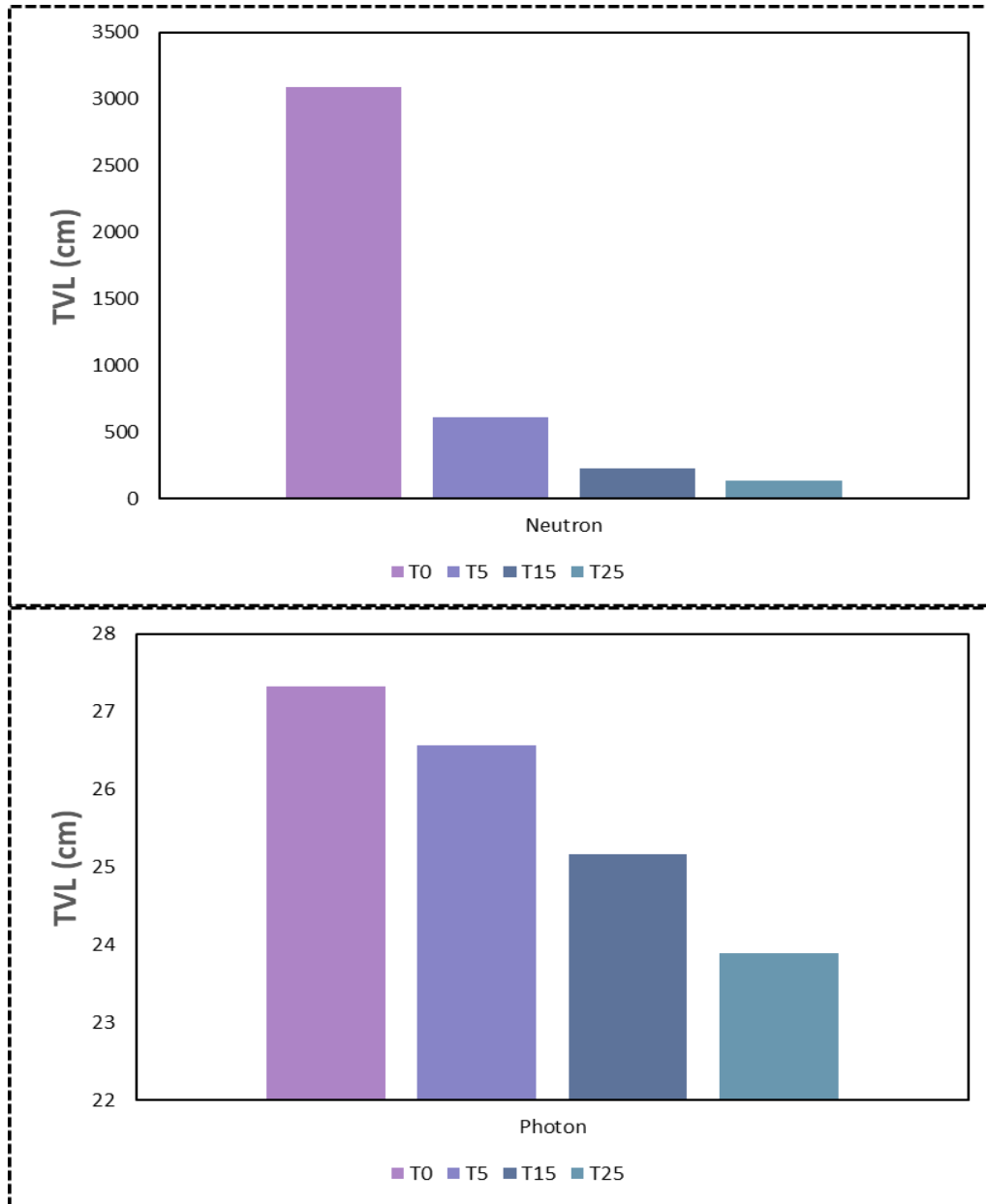


**Figure 3.** TVL graphs of samples coded T0-T5-T15-T25

Neutrons, on the other hand, can pass through many nuclei without losing significant energy before they interact, causing them to travel a longer distance before they are effectively stopped. This has resulted in the difference between the distances required to decrease the density of the incident photon by 90% and the distances required to reduce the intensity of the neutrons by 90%, as shown in Figure 3.

### HVL

The HVL values of the T0-T5-T15-T25 coded samples against photons and fast neutrons with 4 MeV energy are given in Figure 4. Depending on the increasing TiO<sub>2</sub> ratio, the HVL values of the materials against both photons and fast neutrons decrease. The HVL values of the T0-T5-T15-T25 coded samples against fast neutrons are approximately 930.8 cm; 185.6 cm; 67.7 cm; 39.9 cm, respectively. In the photon case, they are approximately 8.2 cm; 7.99 cm; 7.57 cm; 7.19 cm, respectively. The HVL values of the photons are lower because the LAC values of the materials against photons are higher than the LAC values against neutrons. Neutrons have a high ability to penetrate matter, but since they do not experience electromagnetic interactions like gammas, they lose energy at a low rate. For this reason, the distance required to stop neutrons is generally much greater than that of gamma radiation.

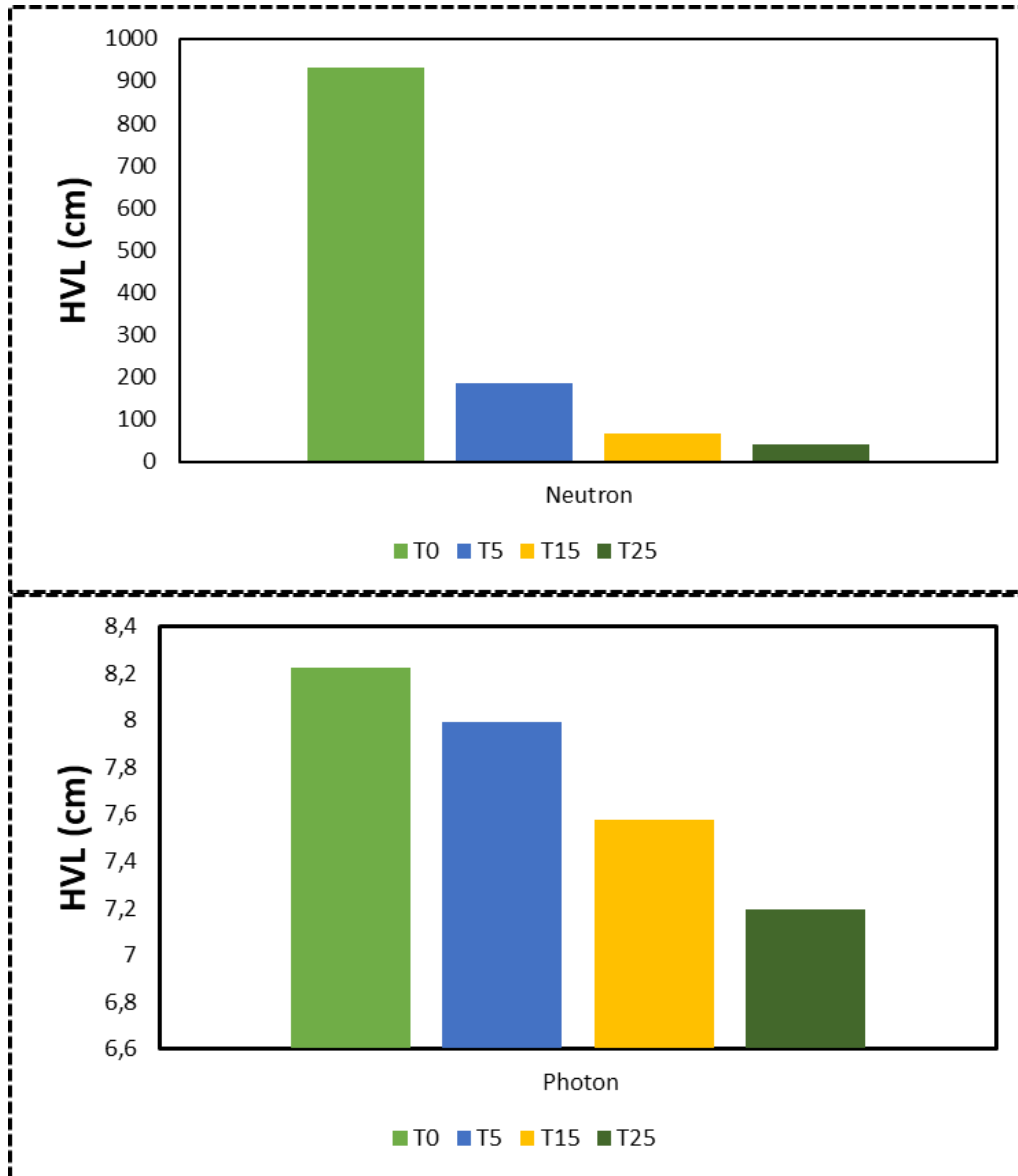


*Figure 4. HVL graphs of samples coded T0-T5-T15-T25*

## MPF

The MPF values of the T0-T5-T15-T25 coded samples against photons and fast neutrons with 4 MeV energy are given in Figure 5. Depending on the increasing doping ratio, there was a rapid decrease in the distance required for the material to make two successive successful collisions with fast neutron particles. There was a reduce in the MPF values against photons with 4 MeV energy. However, it was not as much as the decrease in the distance against fast neutrons. The MPF values of the T0-T5-T15-T25 coded samples against fast neutrons with 4 MeV energy varied between approximately 1343 cm and 58 cm. In the case of photons with 4 MeV energy, it varied between approximately 12 cm and 10 cm. Fast neutrons with energies of 4 MeV can interact by inelastic scattering and elastic scattering. Depending on the type of scattering, this can affect the mean free path. Fast neutrons generally have higher mean free paths in lighter materials because they are less likely to interact with heavier nuclei.

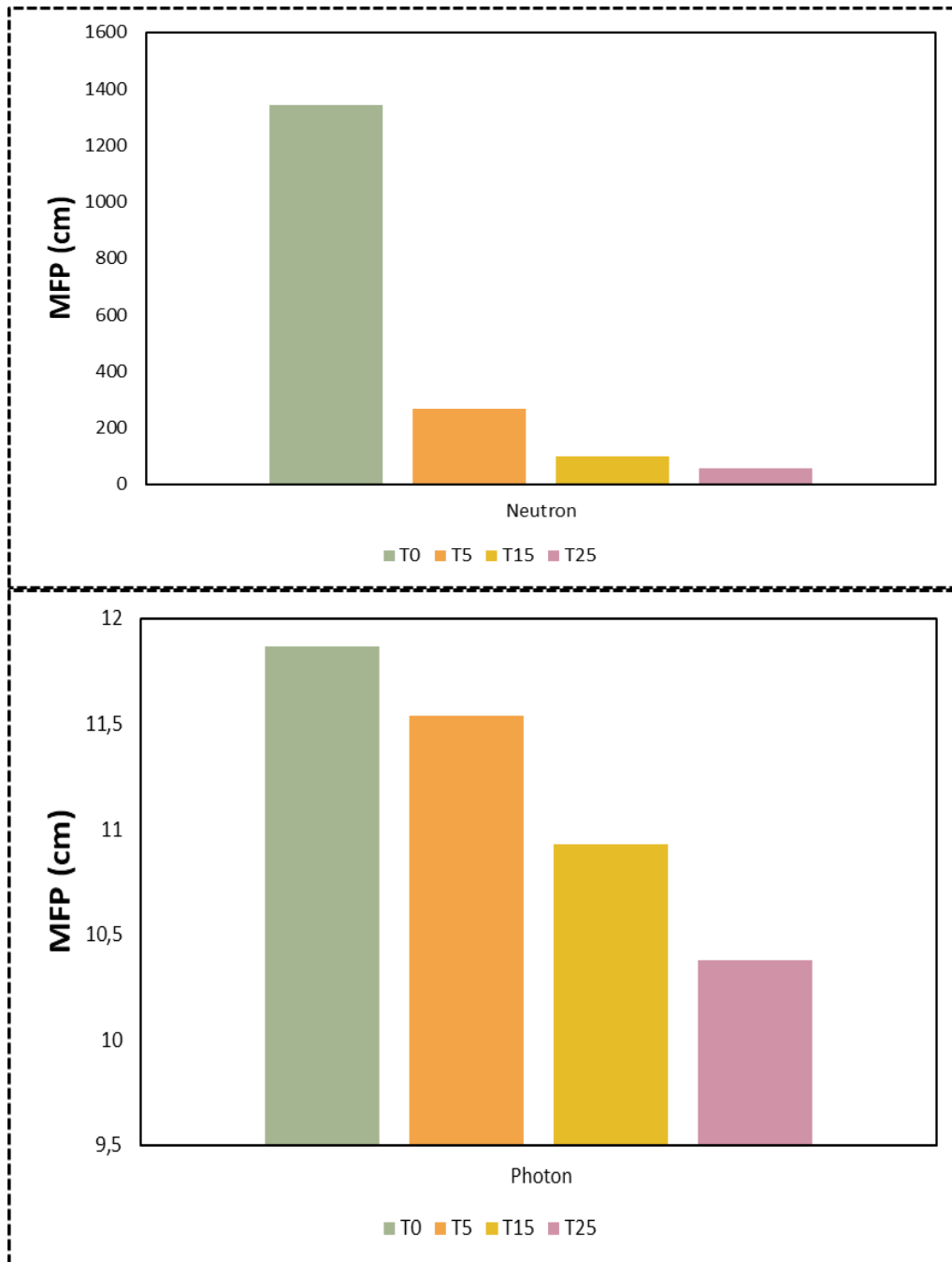


*Figure 5. MFP graphs of samples coded T0-T5-T15-T25*

#### 4. CONCLUSION

The increasing use of artificial radiation (nuclear power plants, hospitals, industry) leads to an increase in the annual dose intake determined by ALARA. This causes many irreversible damages on humans, animals and nature. For this reason, radiation shielding has attracted the attention of many researchers. For this reason, in this study, a study was carried out for a shielding material that can be used for neutron and gamma rays, which are ionising radiations. In this study, MAC, LAC, HVL, MFP and TVL analyses of metal matrix composite materials to which 5-15-25 wt.% TiO<sub>2</sub> ceramic material was added to Al 6082 metal alloy were performed in NGCal program, which provides important information about photon and fast neutron radiations at 4 MeV energy. Among Al 6082, Al 6082+5% TiO<sub>2</sub>, Al 6082+15% TiO<sub>2</sub> and Al 6082+25% TiO<sub>2</sub> samples, Al 6082+25% TiO<sub>2</sub> had the highest high LAC values against fast neutrons and photons, while Al 6082 alloy had the lowest LAC values. While Al 6082 alloy material had the highest HVL values against 4 MeV energy fast neutrons and photons, Al 6082+25% TiO<sub>2</sub> composite material had the lowest HVL



values. The MFP values of the T0-T5-T15-T25 coded samples against fast neutrons with 4 MeV energy varied between approximately 1343 cm and 58 cm. In the case of photons with 4 MeV energy, it varied between approximately 12 cm and 10 cm. By increasing the doping ratio of TiO<sub>2</sub> ceramic material, the photon and fast neutron radiation shielding properties of 4 MeV energy Al 6082 material were improved. The shielding properties of TiO<sub>2</sub> doped metal composites against photons were better than their shielding properties against neutrons.

## ACKNOWLEDGEMENT

The researchers would like to acknowledge the financial support of the Gazi University Scientific Research Projects Office, TÜRKİYE (Project Number: FKA-2023-8617), TÜBİTAK 2211-C Programme and YÖK 100/2000 Programme.

## AUTHOR CONTRIBUTIONS

Conceptualization, Z.Ö and U.G.; methodology, U.G.; fieldwork, Z.Ö.; software, Z.Ö.; title, Z.Ö and U.G.; validation, Z.Ö., and U.G.; laboratory work, Z.Ö.; formal analysis, Z.Ö.; research, Z.Ö.; sources, Z.Ö.; data curation, Z.Ö.; manuscript-original draft, Z.Ö. and U.G.; manuscript-review and editing, Z.Ö and U.G.; visualization, Z.Ö and U.G.; supervision, U.G.; project management, U.G.; funding, Z.Ö. All authors have read and legally accepted the final version of the article published in the journal.

## CONFLICT OF INTEREST

The authors declare no conflict of interest.

## REFERENCES

- Akman, F. Ozkan, I. Kaçal, M. R. Polat, H. Issa, S. A. M. Tekin, H. O. & Agar, O. (2021). Shielding features, to non-ionizing and ionizing photons, of FeCr-based composites. *Applied Radiation and Isotopes*, 167, 109470. <https://doi.org/10.1016/j.apradiso.2020.109470>
- Aldawood, S., Asemi, N. N., Kassim, H., Aziz, A. A., Saeed, W. S., & Al-Odayni, A.-B. (2024). Gamma radiation shielding by titanium alloy reinforced by polymeric composite materials. *Journal of Radiation Research and Applied Sciences*, 17(1), 100793. <https://doi.org/10.1016/j.jrras.2023.100793>
- Alım, B., Ozpolat, O. F., Sakar, E., Han, I., Arslan, I., Singh, V. P., & Demir, L. (2022). Precipitation hardening stainless steels: potential use radiation shielding materials. *Radiation Physics and Chemistry*, 194, 110009. <https://doi.org/10.1016/j.radphyschem.2022.110009>
- Almuqrin, A., Tijani, S. A., Al-Ghamdi, A., Alhuzaymi, T., & Alotiby, F. (2023). Radiation shielding properties of high-density polyethylene (C<sub>2</sub>H<sub>4</sub>)/ molybdenum III oxide (MoO<sub>3</sub>) polymer composites for dental diagnostic applications. *Journal of Radiation Research and Applied Sciences*, 16(4), 100681. <https://doi.org/10.1016/j.jrras.2023.100681>
- Chang, Q., Guo, S., & Zhang, X. (2023). Radiation shielding polymer composites: Ray-interaction mechanism, structural design, manufacture and biomedical applications. *Materials & Design*, 233, 112253. <https://doi.org/10.1016/j.matdes.2023.112253>
- Eke, C. (2024). The role of WO<sub>3</sub> on the optical and radiation attenuation characteristics of ZnO–Na<sub>2</sub>O–B<sub>2</sub>O<sub>3</sub> glasses. *Radiation Physics and Chemistry*, 224, 112036. <https://doi.org/10.1016/j.radphyschem.2024.112036>
- Gökçe, H. S., Güngör, O., & Yılmaz, H. (2021). An online software to simulate the shielding properties of materials for neutrons and photons: NGCal. *Radiation Physics and Chemistry*, 185, 109519. <https://doi.org/10.1016/j.radphyschem.2021.109519>
- Huo, H., Lu, Y., Zhang, H., & Zhong, G. (2024). Sm<sub>2</sub>O<sub>3</sub> micron plates/B4C/HDPE composites containing high specific surface area fillers for neutron and gamma-ray complex radiation shielding. *Composites Science and Technology*, 251, 110567. <https://doi.org/10.1016/j.compscitech.2024.110567>
- Huwayz, M. A., Basha, B., Alalawi, A., Alrowaili, Z. A. Sriwunkum, C., Alsaiari, N. S., & Al-Buriahi, M. S. (2024). Influence of BaO addition on gamma attenuation and radiation shielding performance of SiO<sub>2</sub>-B<sub>2</sub>O<sub>3</sub>-

- SrO-ZrO<sub>2</sub> glasses. *Journal of Radiation Research and Applied Sciences*, 17(4), 101119. <https://doi.org/10.1016/j.jrras.2024.101119>
- Kavun, Y., Kerli, S., Eskalen, H., & Kavgacı, M. (2022). Characterization and nuclear shielding performance of Sm doped In<sub>2</sub>O<sub>3</sub> thin films. *Radiation Physics and Chemistry*, 194, 110014. <https://doi.org/10.1016/j.radphyschem.2022.110014>
- Kılıçoğlu, O., & Tekin, H. O. (2020). Bioactive glasses with TiO<sub>2</sub> additive: behavior characterization against nuclear radiation and determination of buildup factors. *Ceramics International*, 46(8), 10779-10787. <https://doi.org/10.1016/j.ceramint.2020.01.088>
- Jandaghian, B., Dastjerdi, M. H. C., & Mokhtari, J. (2024). Characterization of neutronic parameters and radiation shielding design for an aqueous homogeneous reactor. *Nuclear Engineering and Design*, 417, 112832. <https://doi.org/10.1016/j.nucengdes.2023.112832>
- Juhim, F., Chee, F. P., Awang, A., Moh, P. Y., Salleh, K. A. M., Ibrahim, S., Dayou, J., Alalawi, A., & Al-Buriahi, M. S. (2023). Study of gamma radiation shielding on tellurite glass containing TiO<sub>2</sub> and Al<sub>2</sub>O<sub>3</sub> nanoparticles. *Heliyon*, 9(11), e22529. <https://doi.org/10.1016/j.heliyon.2023.e22529>
- Mahmoud, K. A., Binmujlli, M., Marashdeh, M., Sayyed, M. I., Aljaafreh, M. J., Akhdar, H., Alhindawy, I. G. (2024). Comprehensive analysis of the effects of Mo and Co on the synthesis, structural, and radiation-shielding properties of TiO<sub>2</sub> based composites. *Progress in Nuclear Energy*, 169, 105105. <https://doi.org/10.1016/j.pnucene.2024.105105>
- Nafee, S., Tijani, S. A., Al-Hadeethi, Y., & Hussein, M. A. (2024). Radiation shielding potential of cellulose acetate-CdO-ZnO polymer composites in comparison with concrete and gypsum. *Radiation Physics and Chemistry*, 225, 112145. <https://doi.org/10.1016/j.radphyschem.2024.112145>
- Piotrowski, T. (2021). Neutron shielding evaluation of concretes and mortars: A review. *Construction and Building Materials*, 277, 122238. <https://doi.org/10.1016/j.conbuildmat.2020.122238>
- Reda, S. M., & Saleh, H. M. (2021). Calculation of the gamma radiation shielding efficiency of cement-bitumen portable container using MCNPX code. *Progress in Nuclear Energy*, 142, 104012. <https://doi.org/10.1016/j.pnucene.2021.104012>